

Temperature dependence of the probability of scattering of small groups of electrons in tin and indium

V. A. Gasparov

Institute of Solid State Physics, USSR Academy of Sciences

(Submitted November 29, 1973)

Zh. Eksp. Teor. Fiz. 66, 1492-1500 (April 1974)

The radiofrequency size effect was used to investigate the temperature dependence of the collision frequency ν of small groups of electrons in tin and in indium in the interval 2.3-5.5°K. The scattering probability on the investigated cylindrical sections of the Fermi surfaces of these metals varies with temperature approximately like T^3 . The connection between the collision frequency and the gap between closely-lying sheets of the Fermi surface in amplitude space is analyzed, and it is noted that carrier transfers between these surfaces leads to a complicated temperature dependence of the electron-phonon scattering probability. The results agree with the experimentally observed strong difference between the $\nu(T)$ dependences on Fermi-surface sections with different gap values. The previously observed anomalies in the temperature dependence of the probability of the electron-phonon interaction in indium are explained within the framework of the proposed model.

It is well known that at low temperatures the phonon momentum is much smaller than the Fermi momentum and the frequency of the electron-phonon collisions is proportional to T^3 ^[1]. The geometry of the Fermi surface (FS) exerts a weak influence in this case, since the electron is scattered by the phonon through small angles. However, as shown by Gantmakher, Leonov, and Dologopolov^[2,3], the electron-phonon scattering becomes sensitive to the shape of the FS under conditions when the FS dimensions are small in comparison with the momentum phonon, and we get $\nu \sim T^2$ for a cylindrical surface. This case is realized apparently in bismuth and antimony^[2,3]. A similar behavior of the scattering probability is observed in gallium^[4] and can take place at low temperatures in small groups of electrons in metals, but in this case there is one more circumstance connected with the influence of the FS geometry. Small groups of electrons are located in metals near the principal groups, so that even at low temperatures the electron-phonon interaction can lead to interband transitions of the electrons. Pippard^[5] took into account the contribution of transport processes to the magnetoresistance and has shown that under conditions when the phonon momentum is larger than the gap between the surfaces in momentum space, the transport leads to a T^4 law for the magnetoresistance, owing to the appearance of new electron orbits. The collision frequency should depend on the presence of such transitions, and with decreasing temperature the transport will "die out," and this should lead to a complicated temperature dependence of ν .

THEORETICAL MODEL

It is known^[2] that at a point k on sheet 1 of the FS, located near another sheet (2), the electron collision frequency is given by

$$\nu(k) = \frac{1}{2\pi} \frac{\Delta^2 (k_B T)^2}{\hbar^2 s^2 \mu v_1} [I(0) + \alpha I(x_0)]; \quad (1)$$

$$I(x_0) = \int_0^\infty \frac{x^3 e^x dx}{(e^x - 1)^2}, \quad I(0) = 7.2, \quad \alpha = \frac{v_1}{v_2} \left(\frac{\Delta^*}{\Delta} \right)^2 \left(\frac{s}{s^*} \right)^4$$

μ is the density, k_B is the Boltzmann constant, v_1 and v_2 are the electron velocities on the corresponding FS sheets, and Δ and Δ^* are the deformation-potential constants responsible for the scattering by phonons with velocities s and s^* . The integration variable x is connected with the phonon wave vector q by the relation

$x = \hbar |q| s / k_B T$. The first term in the square brackets in (1) is due to scattering into states on sheet 1 (intra-band scattering), while the second corresponds to transport into states on sheet 2 (interband scattering). Sheets 1 and 2 are separated in momentum space by a gap $\hbar \Delta k$, so that $x_0 = \hbar \Delta k s / k_B T$.

Generally speaking the temperature dependence of ν can be quite arbitrary, depending on the ratio of the quantities in the square brackets of (1), but since $\alpha \gg 1$, the function $\nu(T)$ is determined mainly by the function $I(x_0)$. Indeed, since the electron-phonon interaction matrix elements contain terms of the type e and $k - k'$ ^[1] (e is a unit vector of phonon polarization and $k - k'$ is the change of the electron wave vector as a result of the scattering), it follows that the interband scattering is due to longitudinal phonons with velocity s , since $k - k' = q$. In the case of interband scattering we have $k - k' = q + K$ (K is the distance between the centers of sheets 1 and 2), which is equivalent in some degree to transport processes, therefore the decisive contribution will be made by transverse phonons of velocity s^* . Usually $v_1 \approx v_2$ and $\Delta \approx \Delta^*$, and consequently $\alpha \gg 1$, since $s > s^*$. Figure 1 shows a plot of the integral I against x_0 , obtained with a computer, and shows that the electron-phonon collision frequency at the point k is a complicated function of the temperature. Such a dependence can be observed experimentally by investigating $\nu(T)$ at the turning point of sheet 1 near sheet 2.

In a number of effects, such as ultrasound absorption, cyclotron resonance, or the radio-frequency size effect, one measures the collision frequency averaged over the points on the electron orbit in the magnetic field^[1]:

$$\bar{\nu} = \frac{\hbar}{2\pi m} \oint \frac{\nu(k) dk}{v_\perp}, \quad (2)$$

where m is the cyclotron mass of the electron and v_\perp is the projection of the electron velocity on the plane of the orbit. If the orbit is on sheet 1, then the gap between the surfaces will vary as the electrons move over the orbit. In the model where the orbit is a circle of radius k_0 and the scattering is by a plane of the second surface (see Fig. 2), we have

$$\Delta k = k_0 (\epsilon + 2 \sin^2(\theta/2)), \quad (3)$$

where $\epsilon = \Delta k_0 / k_0$ and Δk_0 is the minimum gap. This formula is valid for transport to a surface located on the right of sheet 1, while the second surface can be easily taken into account by replacing θ with $\pi - \theta$.

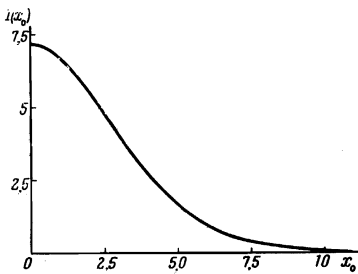


FIG. 1

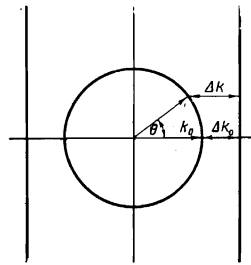


FIG. 2

FIG. 1. The integral I in (1) as a function of the parameter x_0 .
 FIG. 2. Location of the sheets 1 (center) and 2 (right and left) of the FS in the investigated model.

Substituting (3) in (1) and integrating in accordance with (2) we obtain, if v_{\perp} is constant,

$$\bar{v} = \frac{3,6}{\pi} \frac{\Delta^2 (k_B T)^3}{\hbar^2 s^* \mu v_1} \left[1 + \frac{\alpha}{2\pi I(0)} \oint I(x_1) dk \right], \quad (4)$$

$$x_1 = QT^{-1} (\epsilon + 2\sin^2(\theta/2)).$$

Thus, the temperature dependence of \bar{v} is determined by the value of the parameter ϵ and by a certain characteristic temperature $Q = \hbar k_0 s^* / k_B$, at which the transverse-momentum becomes equal to the radius of the orbit. We calculated this dependence with a computer at different values of the parameter ϵ (see Fig. 3); just as the case of the turning point, \bar{v} turned out to be a complicated function of the temperature, approaching asymptotically the T^3 law at high and low temperatures. At $T \gtrsim Q$, according to Gantmakher et al., one should expect the interband-collision to be proportional to T^2 , but the contribution of these collisions to \bar{v} is apparently negligible ($\alpha \gg 1$) and at these temperatures we have $\bar{v} \sim \alpha T^3$.

The relation (4) can be observed experimentally by investigating $\bar{v}(T)$ on sections with different ϵ . We have undertaken an investigation of the temperature dependence of the collision frequency of small groups of electrons (in order to have large ϵ) in tin and in indium, whose FS have been studied in sufficient detail (see, e.g., [6-13]). We investigated the electron and hole surfaces of the third zones of indium and white tin, respectively. The investigations were carried out with the aid of the radio-frequency size effect, which makes it possible to measure the temperature dependence of the collision frequency of the carriers localized on narrow strips on the FS [14].

THE EXPERIMENT

We measured the temperature dependence of the size-effect line amplitudes at 1.5-5.5°K in plane-parallel single-crystal plates of tin with $n \parallel [010]$ and indium with $n \parallel [001]$, with respective thicknesses 0.4 and 0.3 mm. We registered the first ($\partial R / \partial H$) and second ($\partial^2 R / \partial H^2$) derivatives of the active part of the surface impedance of the samples with respect to the magnetic field. The experiments were performed in a field parallel to the surface. The procedure for the measurements and for the reduction of the results are described in [14]. Owing to the smallness of the investigated sections of the FS, the size effect lines were observed in weak fields, where there is a strong nonmonotonic variation of the surface impedance. To exclude this variation when intense lines were recorded, we used the second derivative, but owing to the intensity loss, which

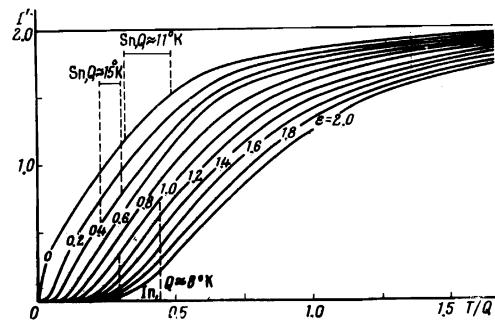


FIG. 3. Temperature dependence of the integral $I' = \int I(x_1) dk / 2I(0)$ in (4) at different values of the parameter ϵ . The dashed lines show the regions of the measurements in tin and indium.

was excessive for the weak line, the nonmonotonic variation of the surface impedance was offset by using also a dc source whose voltage varied nonlinearly with time.

The amplitude of the SE line is connected with the temperature dependent part of the electron collision frequency, averaged over a narrow strip \bar{v} on the FS, with the aid of the rather simple relation [14]:

$$A \sim \exp\left(-\frac{2\pi\gamma}{\Omega} \bar{v}\right), \quad (5)$$

where $\Omega = eH/mc$ is the cyclotron frequency of the electron in the magnetic field H , in which the SE is observed, and γ is a geometric factor that determines which part of the orbit is spanned by the sample thickness ($\gamma = 1/2$ for a circle). Relation (5) is valid under the conditions $\bar{v} + \bar{v}_0 > \Omega$ and $\bar{v}_0 > \bar{v}$, where \bar{v}_0 is the frequency of the collisions with the static defects of the crystal lattice. To verify these conditions we monitored the constancy of the width and shape of the size effect lines over the entire temperature interval.

The size effect in indium has been studied in sufficient detail, so that it was easy to identify the observed lines. Detailed investigations of the anisotropy of the carrier cyclotron masses in tin and indium, carried out by Khaikin and Mina (see, e.g., [10, 13]), make it possible to reconstruct from the experimental size-effect data the temperature dependences of the carrier scattering probabilities, rather than the mean free paths.

TIN

According to the Weitz calculations of the band structure of white tin [9], carried out by the local-pseudopotential method, the tubes δ located on the faces of the Brillouin zone have a shape similar to that of "dog-bones" elongated along the XP axis and located at the points X of the Brillouin zone (Fig. 4). The end faces of the "dog-bones" and their lateral surfaces along XL are in contact with the hole surface in the fourth zone. The gap between the surfaces, which is due to the spin-orbit splitting, is so small that magnetic breakdown takes place, as a result of which orbits are produced that pass through these two surfaces and can be reliably identified in the de Haas-van Alphen effect [8].

The "dog-bone" shape of the surface leads to the appearance of two extremal sections at H parallel to the XP axis. These sections are observed in the size effect [7], in the de Haas-van Alphen effect [8], and in cyclotron resonance [10]. Owing to the peculiar shape of the tubes, there are two strips of effectiveness on the "dog-bone" surface, as a result of which one observes from each section two rather than one size-effect lines,

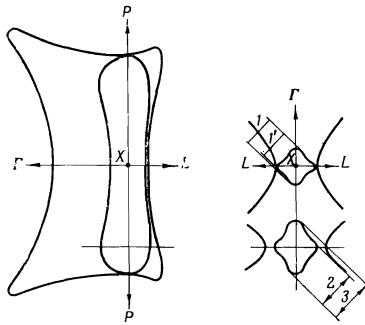


FIG. 4. Arrangements of the tubes δ in the Brillouin zone of white tin. On the right side are separated the central and noncentral sections of the "dog-bone". The numbers label the dimensions of the tubes that determine the size-effect lines.

separated by a certain distance. These lines are due to the one-half and one-quarter electron orbit; in the former case $\gamma = \frac{1}{2}$ and in the latter it can be only stated that γ is close to $\frac{1}{4}$ (see Fig. 4). As a result, lines with $\gamma = \frac{1}{2}$ have a stronger temperature dependence than at $\gamma \approx \frac{1}{4}$.

This circumstance is illustrated clearly in Fig. 5, viz., a rise in temperature leads to the vanishing of the extrema on the right-hand side of the noncentral-section line, whereas the left-hand extrema are reliably observed. The right- and left-hand extrema are responsible here for the size-effect lines with $\gamma = \frac{1}{2}$ and $\gamma \approx \frac{1}{4}$, respectively (see Figs. 4 and 5). For the central section of the contribution of the orbit with $\gamma \approx \frac{1}{4}$ to the size effect is much smaller than that with $\gamma = \frac{1}{2}$. We have therefore investigated for this section only the right-hand most intense part of the line. On the noncentral section, the contributions from each section of the orbit become comparable, but the splitting is much more appreciable, and this makes it possible to investigate both lines.

As seen from Fig. 6, in the entire investigated temperature interval the experimental points fit a T^3 curve, but the deviation of the point from a T^4 law likewise does not exceed the measurement errors. Unfortunately, the limited temperature interval does not make it possible to establish the exponent with sufficient accuracy, but it is seen from Fig. 6 that its value lies between 3 and 4. The dependence of the proportionality coefficients of T^3 on the magnetic-field orientation in the plane of the sample is shown in Fig. 7. The curves 2 ($\gamma \approx \frac{1}{4}$) and 3 ($\gamma = \frac{1}{2}$), it might seem, should coincide, but, as already indicated, in the former case γ is only close to $\frac{1}{4}$, and superposition of the curves yield $\gamma \approx \frac{1}{5}$.

According to Matthey^[7], the gap on the central section is so small that it cannot be reliably determined from experiment ($\epsilon \approx 0$), whereas on the central section we have $\epsilon \approx 0.45$ (see Fig. 4). The characteristic temperatures Q on these sections are $\approx 11^\circ\text{K}$ and $\approx 15^\circ\text{K}$. The velocities of the quasilonitudinal and quasitransverse oscillations, determined from the elastic constants of white tin at helium temperatures^[15], are equal to $s \approx 3.5 \times 10^5$ cm/sec and $s^* \approx 2.0 \times 10^5$ cm/sec.

For a direct comparison of formula (4) with experiment it is necessary to have information on the anisotropy of the Fermi velocity and on the components of the deformation potential. This information is unfortun-

ately missing, but some conclusions can be drawn just the same. From the data of Perz et al.^[16] on the dependence of the area of the extremal sections of the "dog-bone" on the uniaxial and isotropic deformations one can calculate certain components of the deformation potential, averaged over the cross section dimensions:

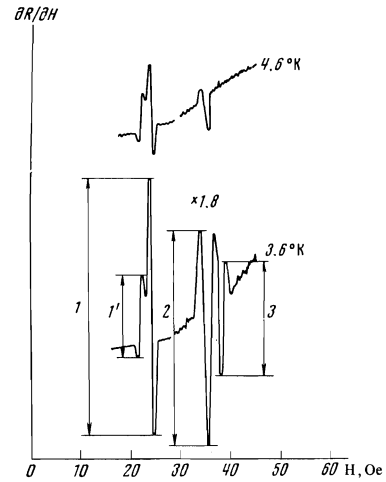


FIG. 5. Typical plot of size-effect lines in tin at two temperatures. The lines in the weaker fields are due to central sections of the tubes, and in stronger fields to the noncentral ones. The arrows mark the dimensions taken to be the amplitudes of the lines, the origin of which is numbered in accordance with Fig. 4. The gain used to record the lines from the central sections was increased 1.8 times, $H \parallel [001]$, $\omega/2\pi = 2.5$ MHz, $d \approx 0.4$ mm.

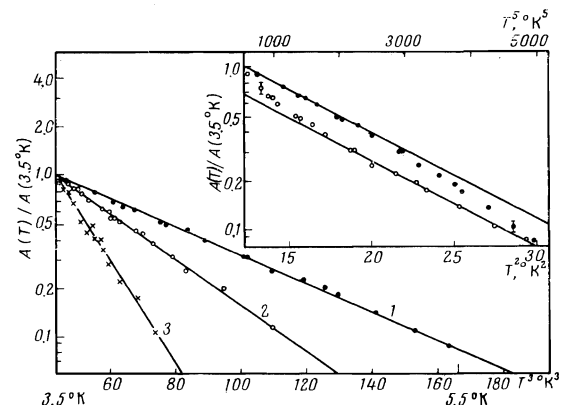


FIG. 6. Temperature dependence of the amplitude of the size-effect lines shown in Fig. 5. The insert shows the dependences on T^2 (●) and T^5 (○) for line 1. The numbers are defined in Fig. 4.

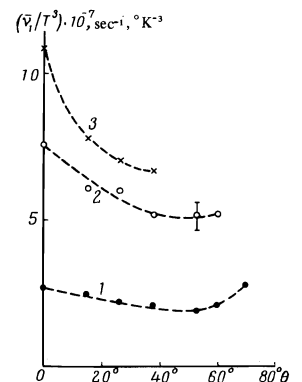


FIG. 7. Anisotropy of the temperature-dependent part of the hole collision frequency on the central (1) and noncentral (2, 3) sections of the tubes δ in the (010) plane. The angle θ is reckoned from the [001] direction.

$$\Delta_{zz} = \frac{\hbar \bar{v}}{2\pi k_0} \frac{\delta A}{\delta p},$$

where δA is the change of the area of the section with radius k_0 under the influence of a relative deformation δp . Estimates show Δ_{zz} to equal 4.2 and 2 eV (the z axis along the "dog-bone" axis) for the central and noncentral sections, respectively. The average diagonal component, on the other hand is equal to 2.0 and 1.5 eV, respectively.

Consequently, the anisotropy of the longitudinal components of the deformation potential cannot explain the experimental data. Indeed, as seen from (4), \bar{v} is determined by the transverse components of the potential ($(s/s^*)^4 \approx 10$), the anisotropy of which is unfortunately not known. In addition, as seen from Fig. 3, the $\bar{v}(T)$ dependence in the investigated region is steeper on the noncentral cross section ($\epsilon \approx 0.45$) than on the central one ($\epsilon \approx 0$), in accord with experiment. It should be noted that what was measured was not $\bar{v}(T)$ itself, but $\bar{v}_1(T) = \bar{v}(T) - \bar{v}(3.5^\circ\text{K})$. Unfortunately, it is impossible to trace the entire temperature region, owing to the superconductivity of the tin, but such investigations are of interest and can be undertaken with the aid of cyclotron resonance.

INDIUM

The electron part of the FS of indium in the third zone takes the form of tubes (β) that are interconnected into quadratic rings^[11-13] (see Fig. 8). The tubes are so arranged that the hole parts of the FS in the second zone are adjacent to them on three sides, so that Umklapp between these surfaces becomes probable. The tubes are nearly triangular in cross section, and the minimum gap between the surfaces, which we determined from the local pseudopotential of Mina et al.^[13], is $\Delta k_0 \approx 0.13 \text{ \AA}^{-1}$ ($k_0 \approx 0.14 \text{ \AA}^{-1}$). The velocities of the quasilongitudinal and quasitransverse oscillations, calculated from the elastic constants of indium at helium temperatures^[17], are respectively $s \approx 2.8 \times 10^5$ and $s^* \approx 0.73 \times 10^5$ cm/sec, and consequently the contribution of the interband transport is larger by approximately two orders of magnitude than that of the interband transitions. In addition, the number of surfaces to which Umklapp can take place as the electron moves along the orbit has increased from two to three in comparison with tin (see Figs. 4 and 8). As a result, the temperature dependence of the integral in (4) changes negligibly in comparison with the $\epsilon = 1$ curve on Fig. 3 (when the limiting value is changed to 3). As seen from the figure, $I \sim T$ in the investigated region, so that one should expect a T^4 law for $\bar{v}(T)$. The experimental points can indeed be fitted to such a law (Fig. 9), but the T^3 is no less suitable. On the orbits that appear when the magnetic field is rotated in the plane of the ring, the temperature dependence of $\bar{v}_1(T) = \bar{v}(T) - \bar{v}(2.3^\circ\text{K})$ decreases and when the angle between the tube axis and the field is 75° the exponent of the power law decreases. This behavior can be attributed to a shift of the corresponding curve on Fig. 3 towards lower temperatures, owing to the decrease of the average gap between the surfaces (see^[12] and Fig. 8).

The orbit on the hole surface in the second zone at $H \parallel [100]$ passes mainly far from the tubes, the contribution of the transport is small, and T^3 in the 1.5–3.5°K interval, with the exponent determined quite accurately in this case. The same law was observed by

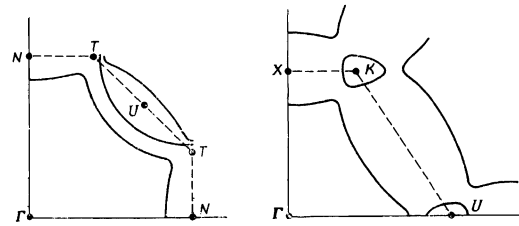


FIG. 8. Intersections of the Fermi surface of indium with the (001) and (110) planes. The surface with center at the point Γ is the hole sheet of the Fermi surface in the second zone. The axes ΓN are directed along [100] and [010], while ΓX is directed along [001].

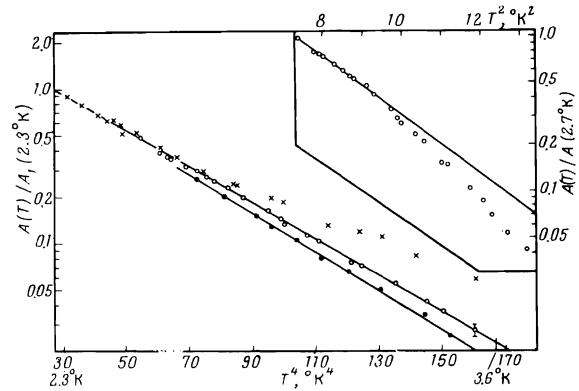


FIG. 9. Temperature dependence of the amplitudes of the size-effect lines of indium at various magnetic-field directions: \bullet — $H \parallel [110]$, \circ — $H \parallel [100]$, $+$ — $\angle H, [110] = 75^\circ$, $\omega/2\pi = 4.2$ MHz, $d \approx 0.3$ mm.

Krylov and Gantmakher in an investigation of the temperature dependence of the mean free path of the electrons on the turning point of the hexagonal "cup" of the hole surface in the second zone at $H \parallel [111]$. In addition, Snyder has observed that \bar{v} for these carriers, on the orbits near the limiting point, increases by a factor of two when the magnetic field is inclined 15° to the [111] direction. This frequency anisotropy of the electron-phonon collisions may be due, within the framework of our model, with the appearance of transport to the tubes β from sections of orbits passing near the edge of the hole surface (see Fig. 8).

Finally, the latest investigations of the electron collision frequency on the central section of the tubes at $H \parallel [110]$, carried out by Castaing and Goy^[20] with the aid of cyclotron resonance, have shown that $\bar{v} \sim T^5$ in the interval 1.5–5.5°K. Indeed, as is clear from Fig. 3, at low temperatures this law follows from the proposed model, albeit at lower temperatures than in^[20]. However, the temperature interval is determined by the parameter Q , which can differ strongly from the $Q \approx 7.8^\circ\text{K}$ used by us, owing to the anisotropy of the phonon spectrum.

It should be noted that all our conclusions are drawn under the assumption that the increment to the electron distribution function is small in comparison with the thermal smearing of the Fermi distribution, i.e., $\hbar\omega \ll k_B T$. In the case of cyclotron resonance this condition is violated and the scattering probability depends on the frequency ω , an increase of which leads to an increase in the number of transports. These effects were indeed observed, it seems, by Castaing and Goy. Of course, the agreement with the predicted behavior of the collision frequency is only qualitative here, since there are too many complicating circumstances to permit direct comparison.

Thus, the electron phonon interaction at low temperatures leads to a complicated temperature dependence of the collision frequency when account is taken of the FS geometry, so that the reduction of the experimental data should be approached with caution. In addition, the described effects uncover very interesting possibilities in the study of the temperature dependence of the collision frequency of small groups of electrons in metals.

The author is grateful to V. F. Gantmakher for interest and critical remarks, to R. N. Gurzhi for a discussion of the result, to I. P. Krylov for supplying the indium samples, and to L. G. Fedyaeva for help with the computer calculations.

¹V. F. Gantmakher, Rep. Prog. Phys. 74, No. 3 (1974).

²V. F. Gantmakher and Yu. S. Leonov, ZhETF Pis. Red. 8, 264 (1968). [JETP Lett. 8, 162 (1968)].

³V. F. Gantmakher and V. T. Dolgoplov, Zh. Eksp. Teor. Fiz. 60, 2260 (1971) [Sov. Phys.-JETP 33, 1215 (1971)].

⁴J. E. Neighbor, C. A. Shiffman, D. G. Chatjigiannis, and S. P. Jacobsen, Phys. Rev. Lett. 27, 929 (1971).

⁵A. B. Pippard, Proc. Roy. Soc. A305, 291 (1968).

⁶V. F. Gantmakher, Zh. Eksp. Teor. Fiz. 44, 811 (1963) [Sov. Phys.-JETP 17, 549 (1963)].

⁷M. P. Matthey, Ph.D. Thesis, University of Mijmegen, 1969.

⁸J. E. Craven and R. W. Stark, Phys. Rev. 168, 849 (1968).

⁹G. Weisz, Phys. Rev. 149, 504 (1966).

¹⁰M. S. Khaikin, Zh. Eksp. Teor. Fiz. 42, 27 (1962) [Sov. Phys.-JETP 15, 18 (1962)].

¹¹V. F. Gantmakher and I. P. Krylov, Zh. Eksp. Teor. Fiz. 49, 1054 (1965) [Sov. Phys.-JETP 22, 734 (1966)].

¹²N. W. Ashcroft and W. E. Lawrence, Phys. Rev. 175, 938 (1968).

¹³M. E. Arustamova, R. T. Mina, and V. S. Pogosyan, Zh. Eksp. Teor. Fiz. 56, 1983 (1969) [Sov. Phys.-JETP 29, 1065 (1969)].

¹⁴V. F. Gantmakher and V. A. Tasparov, Zh. Eksp. Teor. Fiz. 64, 1712 (1973) [Sov. Phys.-JETP 37, 864 (1973)].

¹⁵J. Rayne and B. S. Chandrasekhar, Phys. Rev. 120, 1658 (1960).

¹⁶J. M. Perz, R. H. Hum, and P. T. Coleridge, Phys. Letters 30A, 235 (1969).

¹⁷B. S. Chandrasekhar and J. Rayne, Phys. Rev. 124, 2011 (1961).

¹⁸I. P. Krylov and V. F. Gantmakher, Zh. Eksp. Teor. Fiz. 51, 740 (1966) [Sov. Phys.-JETP 24, 492 (1967)].

¹⁹P. M. Snyder, J. Phys. F.: Metal Phys. 1, 363 (1971).

²⁰B. Castaing and P. Goy, J. Phys. C.: Sol. St. Phys. 6, 2040 (1973).

Translated by J. G. Adashko

154